Deuterium NMR Study of the Structure and Dynamics of the Side Chains of Several Solid Polyglutamates

Eva Meirovitch,[†,‡] Edward T. Samulski,[§] Andrew Leed,[‡] Harold A. Scheraga,*[,‡] S. Rananavare,[‡] George Némethy,[‡] and Jack H. Freed[‡]

Isotope Department, The Weizmann Institute of Science, Rehovot 76100, Israel, Baker Laboratory of Chemistry, Cornell University, Ithaca, New York 14853-1301, and Institute of Material Science, University of Connecticut, Storrs, Connecticut 06268 *(Received: February 10, 1987)*

A ^2H NMR study of polycrystalline powders and oriented films of several selectively deuterium-labeled poly(γ-benzyl L-glutamate) (PBLG) and poly(γ-ethyl L-glutamate) (PELG) homopolymers is reported. The deuterium labels on the ester side chain of PBLG indicate the presence of two polymer species below 330 K, one with benzene rings flipping rapidly about their para axis and the other with benzene rings static on the ^2H NMR time scale. The relative contribution of the "mobile" population increases from about half (55%) at 240 K to nearly total (96%) at 314 K. A phase transition is detected at 330 K. Above this transition temperature, we detect an additional motion consisting of three-site jumps of the benzyl moiety among unevenly populated sites about the O^ϵ–C^ζ bond. Thus the methylene deuterons experience, on the whole, nonaxial symmetry about this bond. At 395 K this motion attains its motional-narrowing limit for all the deuterons that it affects, whereas at 340 K, only 25% of the benzyl moieties are rapidly reorienting, with 75% reorienting at a slower rate. With powders of PBLG labeled selectively at the γ-carbon position, onset of motion at the phase transition is observed. The spectral line shape indicates that, above 330 K, the γ deuteriums experience moderate (at 340 K) to rapid (at 395 K) jumps about the C^β–C^γ bond among three unequally populated sites. The phase transition observed at 330 K, associated with the side-chain melting phenomenon, is likely to be accompanied by rotational or translational diffusion of the helices while they maintain their axial orientation. Furthermore, a comparison with our conformational analysis suggests a high degree of cooperativity between the adjacent helices. At the phase transition, these nearest-neighbor interactions would be reduced, and the NMR results are consistent with computed 3-fold rotational potentials for side-chain motion around the C^β–C^γ and O^ϵ–C^ζ bonds, predicted from the conformational analysis of the side chains attached to the α-helix. With powders and films of PELG, the dominant motion at low temperatures (besides rapid methyl rotation) can be interpreted either as a discrete jump rotation with 3-fold symmetry but about a diffusion axis that does not coincide with the O^ϵ–C^ζ bond, or in terms of a three-site jump motion about this bond among unevenly populated sites. Motional averaging becomes very effective and isotropic in nature at about room temperature. This abrupt change from anisotropic to isotropic motion is indicative of a phase transition. Results obtained with oriented films indicate that the PBLG benzene rings orient preferentially parallel to the axes of the polymer helices, consistent with theoretical predictions, whereas the PELG ethyl groups are distributed randomly in space.

I. Introduction

In order to understand structure–function relationships of biopolymers, it is necessary to have information about the dynamics of local conformational changes in these complex, flexible macromolecules. Various techniques, such as nuclear magnetic resonance (NMR), have been used for this purpose, but the experiments have been carried out primarily in solutions. However, the isotropic motional averaging, because of Brownian reorientation in the liquid state, often limits the acquisition of direct and unambiguous information about internal anisotropic motions and local conformation. On the other hand, by examining these molecules in the solid state, the overall molecular reorientation is impeded, and the internal motions are dominant. Therefore, NMR studies of *solid* polymers provide unique information about local structure and mobility.[1,2] Indeed, recent developments in solid-state NMR methodologies,[3-6] advances in theoretical formulations of dynamic effects on NMR line shapes,[7-17] and progress in the chemistry of selective isotopic labeling have pointed out the value and potential of high-resolution, dynamic, solid-state NMR.[1,2,18-30] At the same time, these reports have also made clear the inherent limitations due to spectral sensitivity and resolution, as well as sample morphology. Analogous to X-ray crystallography, the information provided by single-crystal experiments is superior in quality, and far more extensive, than that obtained with polycrystalline powders. Since the demands on the dimensions of single crystals appropriate for NMR experiments are quite stringent, most previous workers have studied only polycrystalline powders.[1-6,18-30]

In this work, we report the results of NMR experiments performed on partially oriented solid structures derived from liquid crystalline phases. When these rodlike chiral (right-handed α-helical) poly(amino acid) derivatives are solubilized in helicogenic

[†] The Weizmann Institute of Science.
* Author to whom correspondence should be addressed.
[‡] Cornell University.
[§] University of Connecticut.

(1) Hentschel, D.; Sillescu, H.; Spiess, H. W. *Macromolecules* **1981**, *14*, 1605.
(2) Jelinski, L. W.; Dumais, J. J.; Watnick, P. I.; Engel, A. K.; Sefcik, M. D. *Macromolecules* **1983**, *16*, 409 and references cited therein.
(3) Mehring, M. *High Resolution NMR Spectroscopy in Solids*, 2nd ed.; Springer-Verlag: New York, 1983.
(4) Haeberlen, U. *High Resolution NMR in Solids*; Academic: New York, 1976.
(5) Skarjune, R.; Oldfield, E. *Biochemistry* **1979**, *18*, 5903.
(6) Griffin, R. G. *Methods Enzymol.* **1981**, *72*, 108.
(7) Freed, J. H.; Bruno, G. V.; Polnaszek, C. F. *J. Phys. Chem.* **1971**, *75*, 3385.
(8) Baram, A.; Luz, Z.; Alexander, S. *J. Chem. Phys.* **1973**, *58*, 4558.
(9) Alexander, S.; Baram, A.; Luz, Z. *J. Chem. Phys.* **1974**, *61*, 992; *Mol. Phys.* **1974**, *27*, 441.
(10) Mason, R. P.; Polnaszek, C. F.; Freed, J. H. *J. Phys. Chem.* **1974**, *78*, 1324.
(11) Spiess, H. W. *Chem. Phys.* **1974**, *6*, 217.
(12) Spiess, H. W.; Grosescu, R.; Haeberlen, U. *Chem. Phys.* **1974**, *6*, 226.
(13) Baram, A.; Luz, Z.; Alexander, S. *J. Chem. Phys.* **1976**, *64*, 4321.
(14) Alexander, S.; Luz, Z.; Naor, Y.; Poupko, R. *Mol. Phys.* **1977**, *33*, 1119.
(15) Pschorn, O.; Spiess, H. W. *J. Magn. Reson.* **1980**, *39*, 217.
(16) Campbell, R. F.; Meirovitch, E.; Freed, J. H. *J. Phys. Chem.* **1979**, *83*, 525.
(17) Meirovitch, E.; Freed, J. H. *Chem. Phys. Lett.* **1979**, *64*, 311.
(18) Davis, J. H.; Jeffrey, K. R.; Bloom, M.; Valic, M. I.; Higgs, T. P. *Chem. Phys. Lett.* **1976**, *42*, 390.
(19) Bloom, M.; Davis, J. H.; Valic, M. I. *Can. J. Phys.* **1980**, *58*, 1510.
(20) Huang, T. H.; Skarjune, R. P.; Wittebort, R. J.; Griffin, R. G.; Oldfield, E. *J. Am. Chem. Soc.* **1980**, *102*, 7377.
(21) Wittebort, R. J.; Schmidt, C. F.; Griffin, R. G. *Biochemistry* **1981**, *20*, 4223.
(22) Jacobs, R. E.; Oldfield, E. *Prog. Nucl. Magn. Reson. Spectrosc.* **1981**, *14*, 113.
(23) Rice, D. M.; Wittebort, R. J.; Griffin, R. G.; Meirovitch, E.; Stimson, E. R.; Meinwald, Y. C.; Freed, J. H.; Scheraga, H. A. *J. Am. Chem. Soc.* **1981**, *103*, 7707.
(24) Wittebort, R. J.; Blume, A.; Huang, T. H.; DasGupta, S. K.; Griffin, R. G. *Biochemistry* **1982**, *21*, 3487.

0022-3654/87/2091-4840$01.50/0

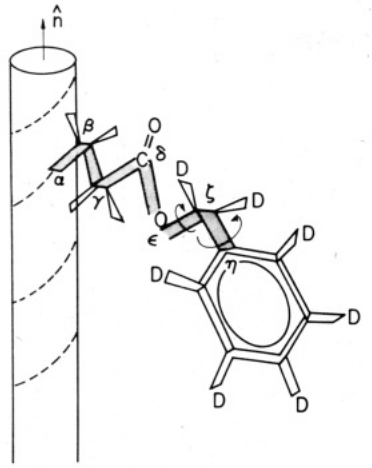

Figure 1. Schematic drawing of PBLG. The C^α of the glutamic acid residue forms part of the helical backbone. The side chain consists of the β-, γ-, and δ- (carbonyl) carbons of the glutamic acid residue, the ϵ-oxygen, the ζ-carbon, the benzene ring of the benzyl ester group, with attached hydrogens, and the carbonyl O. The orientation of the side chain relative to the helix axis ($\hat{n}$) in this drawing is arbitrary. The labeling corresponds to PBLG-d_7.

solvents (chloroform, dioxane, etc.), twisted nematic (cholesteric) liquid crystalline phases form at high polymer concentrations ($\gtrsim$15 wt % concentration).[31] In these phases, one may define a local nematic director for each region in which the helix axes are nearly parallel. It is the direction of preferential alignment of the helix axes. Macroscopically aligned samples can be prepared by subjecting the liquid crystal to magnetic (or electric) fields. In such samples, the diamagnetic (dielectric) susceptibility is positive, and each local director now becomes aligned parallel to the direction of the applied field. These properties have been used previously to fabricate oriented, uniaxial, solid poly(amino acid) films.[32] The resulting array of parallel helices is sufficiently uniform for molecular structural studies by X-ray diffraction;[33] this magnetic orientation technique was subsequently extended to liquid-crystal-forming viruses.[34] We have used this technique to prepare partially oriented films of poly(γ-benzyl L-glutamate) (PBLG) and poly(γ-ethyl L-glutamate) (PELG). The covalent structure of PBLG is illustrated schematically in Figure 1. PELG has a similar structure, with the benzyl ester group replaced by an ethyl ester group.

The purpose of this work is to elucidate the structure and dynamics of the side chains of the α-helix in solid, selectively deuteriated poly(amino acid) derivatives by NMR. We also illustrate the value of using ordered morphologies to study dynamics and structure.[35,36]

II. Experimental Section

Preparation of Deuterium-Labeled PBLG Polymers. The preparation of specifically labeled PBLG (PBLG-d_1 and PBLG-d_7) has been described previously;[37] the former has deuterium in the para position of the benzene ring and the latter is deuteriated in the seven positions shown in Figure 1. PBLG-$d_2(\gamma)$, with deuterium in the two γ positions (Figure 1), was kindly given to us by Dr. Kuniaki Nagayama, University of Tokyo. Since glutamic acid-$d_2(\gamma)$ is available commercially,[38] PBLG-$d_2(\gamma)$ could be synthesized by the same procedures outlined below for the preparation of the PBLG polymers.

Preparation of Deuterium-Labeled PELG Polymers. Reagents. Bromoethane-*2,2,2-d*$_3$ and bromoethane-*1,1-d*$_2$, >98% isotopic purity, were obtained from Merck Sharp & Dohme. Trichloromethyl chloroformate was purchased from Alpha Products. Dioxane was distilled from sodium under nitrogen immediately before use.

Sodium copper L-glutamate was prepared previously in our laboratory by the method of Ledger and Stewart.[39]

γ-(Ethyl-*2,2,2-d*$_3$) L-glutamate was synthesized by dissolving bromoethane-*2,2,2-d*$_3$ (2 equiv) and sodium copper L-glutamate (1 equiv) in 50:50 dimethylformamide–water (2.5 mL of mixture/mmol of $BrCH_2CD_3$). This mixture was heated to 50 °C in a sealed tube for 48 h. After the solvent was removed in vacuo, the whole residue was dissolved in hot H_2O. Saturation with H_2S gave a precipitate of CuS which was removed by filtration. The solution was adjusted to pH 5.5 by using CH_3COOH and NH_4OH and loaded onto a Dowex-1 column (acetate form). The ethyl glutamate was collected immediately following the void volume, eluting with 50 mM ammonium acetate. The eluant was adjusted to pH 4.6 and loaded onto a Dowex-50 column (ammonium form). The ethyl glutamate was collected by eluting with 50 mM ammonium acetate, pH 4.6. Repeated lyophilization to constant weight (to remove ammonium acetate) gave a 48% yield of γ-(ethyl-*2,2,2-d*$_3$) L-glutamate: mp 193–194 °C, pure by silica gel TLC; R_f = 0.49 (4:3:3 butanol–CH_3COOH–H_2O).

γ-(Ethyl-*2,2,2-d*$_3$) L-glutamate *N*-carboxyanhydride (NCA) was synthesized by treating γ-(ethyl-*2,2,2-d*$_3$) L-glutamate with 0.6 equiv of trichloromethyl chloroformate in dioxane (10 mL/mmol of ethyl glutamate). The solution was stirred under nitrogen at 60 °C for 4 h and then cooled to 40 °C. The ethyl glutamate was added, and stirring continued until the suspension dissolved. The solvent was removed in vacuo, and the residue was triturated twice with hexane. Crystallization from ether–hexane gave a 95% yield: mp 71.5–72.5 °C.

Poly[γ-(ethyl-*2,2,2-d*$_3$) L-glutamate] (PELG-d_3) was formed from the NCA by using sodium methoxide as a polymerization initiator. γ-(Ethyl-*2,2,2-d*$_3$) L-glutamate NCA was dissolved in dioxane (40 mL/g of NCA) under nitrogen. Sodium methoxide in 50:50 methanol–benzene was added to give an NCA/initiator ratio of 70. After stirring overnight, the solution was poured slowly into a stirring solution of 50:50 methanol–water (10 mL/mL of dioxane). The polymer was allowed to settle, and the solvent was decanted off and renewed with a fresh batch. This cycle was repeated 4 times (to remove dioxane), and the fibrous polymer was collected by filtration and vacuum dried to give an 81% yield.

Poly[γ-(ethyl-*1,1-d*$_2$) L-glutamate] (PELG-d_2) and its precursors were prepared by identical methods as above, with similar yields and purity.

Preparation of Samples for NMR Experiments. The polycrystalline powders of PBLG-d_1 and PBLG-d_7 were compacted in 5-mm o.d. tubes, 1 cm in length. Those of PBLG-$d_2(\gamma)$, PELG-d_3, and PELG-d_2 were compacted in 10-mm o.d. tubes, 1.5 cm in length.

The PBLG-d_7, PELG-d_3, and PELG-d_2 films were prepared by casting (slowly evaporating) liquid crystalline solutions on a mercury surface in a 20-kG magnetic field as described in ref 32. The NMR experiments on oriented samples utilized circular segments ($\sim$1 cm in diameter) cut from cast polymer films ($\sim$1 mm in thickness). X-ray diffraction (Cu Kα irradiation, flat film) was used to determine sample homogeneity and to establish the orientation of the director (optical axis) and the degree of orientational order. As reported earlier,[40] azimuthal diffraction

(25) Meirovitch, E.; Krant, T.; Vega, S. *J. Phys. Chem.* **1983**, *87*, 1390.
(26) Jelinski, L. W.; Dumais, J. J.; Engel, A. K. *Macromolecules* **1983**, *16*, 403 and references cited therein.
(27) Jelinski, L. W.; Dumais, J. J.; Engel, A. K. *Macromolecules* **1983**, *16*, 492.
(28) Schaefer, J.; Stejskal, E. O.; McKay, R. A.; Dixon, W. T. *J. Magn. Reson.* **1984**, *57*, 85.
(29) Jelinski, L. W.; Dumais, J. J.; Cholli, A. L. *Polym. Prepr. (Am. Chem. Soc., Div. Polym. Chem.)* **1984**, *25*, 1.
(30) Frey, M. H.; Opella, S. J.; Rockwell, A. L.; Gierasch, L. M. *J. Am. Chem. Soc.* **1985**, *107*, 1946.
(31) Samulski, E. T. In *Liquid Crystalline Order in Polymers*; Blumstein, A., Ed.; Academic: New York, 1978; Chapter 5.
(32) Samulski, E. T.; Tobolsky, A. V. *Macromolecules* **1968**, *1*, 555.
(33) Samulski, E. T.; Tobolsky, A. V. *Biopolymers* **1971**, *10*, 1013.
(34) Nave, C.; Fowler, A. G.; Malsey, S.; Marvin, D. A.; Siegrist, H. *Nature (London)* **1979**, *281*, 232.
(35) Samulski, E. T. *Polymer* **1985**, *26*, 177.
(36) Cross, T. A.; Tsang, P.; Opella, S. J. *Biochemistry* **1983**, *22*, 721.
(37) Kwiatowski, J. Masters Dissertation, University of Connecticut, 1978.
(38) Merck, Sharp & Dohme, Montreal, Canada.
(39) Ledger, R.; Stewart, F. H. C. *Aust. J. Chem.* **1965**, *18*, 1477.

intensity with the director perpendicular to the incident X-ray beam yields high orientational order parameters ($S > 0.95$), i.e., nearly perfectly parallel α-helices. In recent studies,[41] the diffraction pattern observed with the beam *parallel* to the director indicates long-range (macroscopic) hexagonal packing of the helices throughout the magnetically oriented films. In spite of the good lateral packing of the helices, there is little evidence for longitudinal, crystallike registration of the side chains in the diffraction patterns.[42] Thus, the term *paracrystal* seems to be the best characterization of the highly ordered hexagonal array of helices in such films.

The ^{2}H NMR experiments were performed on the Bruker CXP-300 spectrometer of the Isotope Department, The Weizmann Institute of Science, Rehovot, Israel. The deuterium Larmor frequency was 46.07 MHz, and a horizontal solenoid coil high-power probe was used. All ^{2}H NMR spectra were obtained with the quadrupole echo pulse sequence ($90_{\pm x}$, τ_e, 90_y, t) experiment with a delay time of τ_e = 20–30 μs and a 90° pulse of 3.3 μs with the commercial 5-mm-o.d. high-power ^{2}H probe and 7.4 μs with the commercial 10-mm-o.d. high-power ^{2}H probe. The quadrature-detected echo signal obtained at $t = 2\tau_e$, following the first pulse, was Fourier transformed. Instrumental artifacts due to finite pulse length, typically encountered,[19] do not affect our conclusions, except for near-rigid-limit spectra recorded with the 10-mm-o.d. probe employing a 90° pulse width of 7.4 μs. The rigid-limit deuterium spectra have typical spectral widths on the order of 250–280 kHz. Thus, the pulse length used with the 10-mm probe causes extensive amplitude distortions in the deuterium NMR line shapes. We shall comment upon these artifacts at appropriate places where these distortions affect the comparisons with simulated spectra.

Spectra were typically obtained with 1000–5000 accumulations with a repetition time of 1–2 s. In experiments carried out to assess the effects of a finite delay time τ_e, it was varied between 20 and 100 μs but no significant line shape distortions were observed. Repetition times were chosen so as to avoid spectral distortions due to T_1 anisotropy.

The NMR spectra were found to be insensitive to decoupling of protons in the same molecule, using the maximum power (20 W) achievable with the 5-mm probe.

The temperature at the sample was controlled with a flow of nitrogen gas and stabilized with a temperature control unit with a precision of roughly ±1 °C.

III. Theoretical Background

The main anisotropic term in the spin Hamiltonian for a deuterium nucleus in a solid is the quadrupole interaction.[3,43] Assuming, for the sake of simplicity, that the quadrupole tensor is axially symmetric,[44] the NMR spectrum of a carbon-bound deuterium atom, with the C–D bond oriented at a unique angle θ with respect to the external field H_0, is a doublet with a splitting[3,43] (in kilohertz) of

$$\Delta\nu = (3e^2qQ/4h)(3\cos^2\theta - 1) \quad (1)$$

The quantity e^2qQ/h is the quadrupole coupling constant Q_0 of the axial tensor $\mathbf{Q}_0$. For a polycrystalline sample (with C–D bonds at various orientations θ), the spectrum will be given by a properly weighted superposition of doublets, resulting in a typical pattern such as that illustrated in Figure 2A (obtained with Q_0 = 165 kHz and a "natural line width" T_2^{*-1} = 0.21 kHz). The spectrum is symmetric about the Larmor frequency ν_0, and the dominant

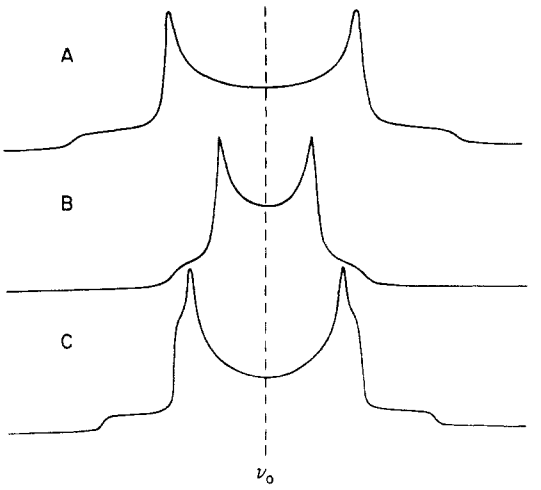

Figure 2. (A) Axial rigid-limit powder spectrum [i.e., a properly weighted (sin θ dθ) superposition of doublets] obtained with a quadrupole coupling constant Q_0 = 165 kHz and a natural line width T_2^{*-1} = 0.21 kHz; ν_0 denotes the position of the Larmor frequency. (B) Partially averaged powder spectrum obtained by allowing the C–D bond associated with spectrum A to spin rapidly about a diffusion axis orthogonal to the C–D bond [i.e., α = 90° and $|(1/2)(3\cos^2\alpha - 1)| = 0.5$]. (C) Asymmetric rigid-limit powder spectrum obtained with Q_0 = 165 kHz, η^* = 0.21, $T_2^{*-1}(x) = T_2^{*-1}(y)$ = 2.4 kHz and $T_2^{*-1}(z)$ = 4.7 kHz.

features of this line shape are two strong peaks disposed symmetrically about ν_0 and separated by $\delta_0 = (3/4)Q_0$ (=124 kHz) and two extreme shoulders separated by $2\delta_0$; the former corresponds to θ = 90° orientations (we shall refer to these as the "perpendicular peaks") and the latter to θ = 0° orientations (to be called the "parallel peaks"). (Note that a Q_0 = 165 kHz applies in this work to aliphatic deuterons, while Q_0 = 184 kHz applies to aromatic deuterons.[2])

The spectrum just described is a rigid-limit axial powder spectrum. With the onset of motion, the C–D bonds will span the various orientations in space in a manner determined by the nature of the dynamic process, and the line shape will alter accordingly. In principle, the type of motion, the symmetry and magnitude of local orienting potentials, as well as geometric features such as tilt angles between diffusion and magnetic axes, can be derived from an analysis of the spectrum.[7,15,17] A simple example, relevant to the forthcoming discussion, is that of *rapid* reorientation about a diffusion axis tilted at an arbitrary angle α relative to the C–D bond. Should this motion be uniformly diffusive or should the molecule execute discrete jumps between equivalent sites of symmetry equal to or higher than C_{3v}, partial averaging of the original tensor $\mathbf{Q}_0$ to an effective axially symmetric tensor $\mathbf{Q}$, with its principal axis z' along the diffusion axis, will occur in the fast motional limit.[7,15,17] The principal value Q can be calculated straightforwardly from those of Q_0 and the orientation of the diffusion axis in the local frame of the latter, and vice versa; i.e., given Q, one can derive geometric parameters. With a polycrystalline sample, one would therefore expect a pattern analogous to a true rigid-limit (static) powder spectrum, but reduced along the frequency axis by the factor $(1/2)(3\cos^2\alpha - 1)$ [i.e., $Q = Q_0(1/2)(3\cos^2\alpha - 1)$, as illustrated in Figure 2B for α = 90°].

For *slower* motions, the NMR spectrum is sensitive to the model, and the appearance of the spectrum will depend on the gradually changing motional rates. It typically will be different for discrete C_{3v} jumps compared to continuous diffusion.[7,15,17]

Since the quadrupole tensor is traceless, isotropic motion (i.e., reorientation about all angles in the unit sphere) will lead to a complete collapse of the quadrupole structure to give, in the fast motional limit, a single line centered at ν_0. (It should be noted, however, that, for reorientation about a unique axis, a similar spectrum will result if α = 54.7°, the so-called "magic angle", for which $3\cos^2\alpha - 1 = 0$).

A relevant extension of the simple considerations outlined above relates to *nonuniform* reorientation about a unique diffusion axis.

(40) Murthy, N. S.; Knox, J. R.; Samulski, E. T. *J. Chem. Phys.* **1976**, *65*, 4835.
(41) Murthy, N. S.; Samulski, E. T.; Knox, J. R. *Macromolecules* **1986**, *19*, 941.
(42) Lefelar, J. A.; Knox, J. R.; Samulski, E. T. *Biopolymers* **1983**, *22*, 1071.
(43) See, for example, Hsi, S.; Zimmermann, H.; Luz, Z. *J. Chem. Phys.* **1978**, *69*, 4126 and references cited therein.
(44) The quadrupole tensor has principal axes x, y, and z and principal values V_{xx}, V_{yy}, and V_{zz}. For an axially symmetric tensor V_{xx} equals V_{yy}; i.e., the asymmetry parameter η = 0, where η is defined as $(V_{xx} - V_{yy})/V_{zz}$ with $|V_{zz}| > |V_{xx}| > |V_{yy}|$.

In general, in the fast motional limit, such a process will lead to an asymmetric, rather than an axially symmetric, powder pattern. Such a powder spectrum is shown in Figure 2C. If one can specify the nature of this nonuniformity, the line shape can be predicted, (but not necessarily vice versa).

In the following presentation, we shall refer repeatedly to partially averaged axial powder spectra obtained as a result of fast reorientation about internal diffusion axes. In many cases, Q will be determined directly from the fast motional experimental spectrum by measuring the distance δ between the perpendicular peaks. Should the molecule under investigation contain several (n) nonequivalent C–D bonds [in the sense that they have identical quadrupole constants Q_0 but different orientations α_i ($i = 1-n$) relative to the internal diffusion axis], the ^{2}H NMR spectrum will consist of a superposition of the n powder spectra. The potential for obtaining conformational characteristics is obvious.

A. 180° Jumps of a C–D Bond about a Unique Diffusion Axis. This model is treated in great detail in ref 3, and we shall briefly summarize here only the main features. This motion can easily be identified as a jump between two sites for the C–D bond. In the fast motional limit (jump rate $\gg 10^6$ s^{-1}) one can simply average the resonance frequency of the spin-label in the two sites to determine the powder line shape, shown in Figure 2C. This is a simple calculation keeping only the secular form in the quadrupolar Hamiltonian.

It is also possible to evaluate the powder spectrum for the case of biased reorientation, i.e., for a case in which the occupational probabilities for the two sites are not equal. In simulating the experimental spectra, the population ratio will be denoted by R.

B. 120° Jumps of a C–D Bond about a Unique Diffusion Axis. The calculation of ^{2}H NMR line shapes for *rapid* 120° jumps of C–D bonds (e.g., those of a methyl group) about a unique jump axis is based on a standard formulation.[16,45,46] In all such calculations, we used 1600 orientations of the jump axis. Simulations were performed on an IBM-PC. A Basic precompiled program ran typically for 25 min. The slow motional spectra were calculated by using 10 000 orientations to simulate the powder averaging.

C. Combined Motions. Finally, should the diffusion axis itself undergo additional motions, the spectrum will be further averaged. We shall consider a simplified model, wherein the combined effect of several dynamic processes can be substituted by a diffusive or jump-type motion about a unique diffusion axis,[16] or else by rapid libration of a unique diffusion axis within a cone centered at a given orientation in space. The axial powder pattern, obtained in the absence of libration, will be further averaged (by the libration) to another axial powder pattern of reduced width; we denote, by a scaling parameter $0 \leq \Delta \leq 1$, the extent to which the overall width is reduced. An order parameter S, similar to the parameter used to estimate ordering in anisotropic fluids,[43] can be defined as the ratio of the perpendicular peak separation in the presence and in the absence of anisotropic motion (e.g., libration).

IV. Results and Discussion

A. Poly(γ-benzyl L-glutamate) (PBLG). 1. PBLG Labeled at the Ester Position: PBLG-d_7 and PBLG-d_1. ^{2}H NMR spectra of PBLG-d_7 and PBLG-d_1 powder samples obtained at various temperature are shown in Figures 3A and 4A, respectively. The 293 K spectrum of the latter and the 140 K spectrum of the former are rigid-limit spectra with a separation of roughly 130 kHz between the perpendicular peaks (the parallel peaks are lost in the noise), indicating that a large fraction of deuterons are immobile on the ^{2}H NMR time scale at those temperatures. The PBLG-d_7 spectrum alters dramatically upon increasing the temperature from 140 to 297 K, then changes gradually from 297 K to slightly below 330 K, but changes abruptly from a structured pattern below 330 K into a symmetric structureless line above 330 K, centered at the Larmor frequency. The 330 K spectrum

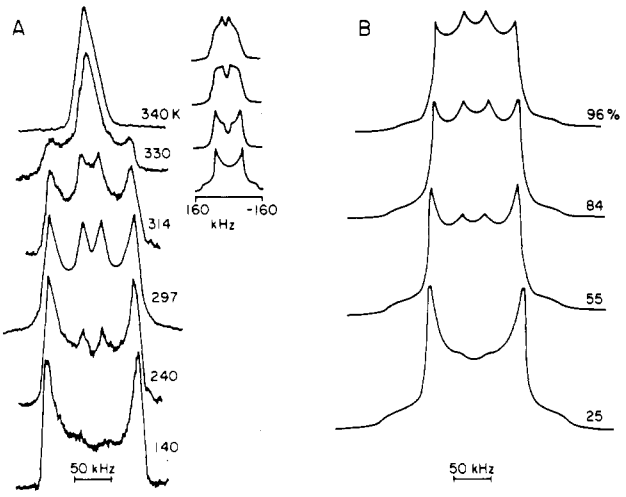

Figure 3. (A) Experimental ^{2}H NMR spectra obtained from a powder sample of PBLG-d_7 at the temperatures indicated. (Inset) Spectra calculated for 180° jumps with $Q_0 = 178.7$ kHz, $\tau^{-1} = 10^5$ s^{-1}, $\alpha' = 60°$, $R = 1$, $T_2^{*-1} = 0.02$ (expressed in units of Q_0), and $\tau^{-1} = 1.0 \times 10^3$, 5.6×10^4, 4.0×10^5, and 1.3×10^6 s^{-1}, respectively, from bottom to top. (B) Mixtures of the simulated fast (jump rate 1.25×10^7 s^{-1}) and rigid-limit spectra for PBLG-d_7. The line width used is 3% of the Q_0 value. The numbers adjacent to the curves indicate the percentages of mobile aromatic rings.

is apparently a two-phase pattern. For PBLG-d_1, a true rigid-limit pattern is observed up to 330 K (not shown), where again an abrupt change occurs.

These general observations suggest that a phase transition occurs at approximately 330 K in the PBLG polymers. Additionally, the NMR spectra of PBLG-d_7 indicate that the seven deuterium labels are each affected in a different manner below the transition. Indeed, we expect the benzene ring to be the most mobile moiety of the PBLG side chain (cf. Figure 1), and the most likely motions that one would associate with it are ring flips.[23] In the inset of Figure 3A, we show ^{2}H NMR spectra calculated for 180° jumps about the C^ζ–C^η axis of the benzene ring; these spectra are associated with aromatic deuterons located off the jump axis for the motional rates denoted in the figure caption.

It should be noted that only *four deuterons* (the two pairs of ortho and meta deuterons) will "sense" this motion, whereas the ^{2}H NMR spectra of the remaining *three deuterons* [the *para* deuteron (located on the jump axis) and the methylene deuterons] will be insensitive to the flipping of the benzene ring; in the absence of additional motion, the *para* and the two methylene deuterons will generate a rigid-limit spectrum. With the four *meta* and *ortho* deuterons generating dynamic spectra, of the type illustrated in the inset of Figure 3A, the overall line shape will be a superposition of the two components. Indeed, the intriguing feature for the series of spectra between 240 and 314 K is the appearance of a fast motional spectrum of monotonically increasing intensity, due to the meta and ortho deuterons, superimposed on a rigid spectrum. Nowhere during this sequence of temperatures do we see spectra identical with the (simulated) slow motional spectra depicted in the inset of Figure 3A. In order to obtain a further understanding, albeit a qualitative one, of this "rigid-amorphous" characteristic of the polymer, we investigated the spectral consequences of mixing the fast motional spectrum of ring deuterons (ortho and meta) and the rigid-limit spectrum for the methylene and para deuterons. We found, however, that a good fit with the experimental data can be obtained only if we assume that a certain percentage of the benzene rings are immobile. A comparison of the simulations shown in Figure 3B with the experimental results in Figure 3A yields 96, 84, and 55% mobile benzene rings from the 314, 297, and 240 K spectra, respectively, with a ±5% error. Also, at 140 K the spectrum displays the hints of a combination of a slow motional spectrum (the third simulated spectrum from the top in the inset of Figure 3A) with a rigid-limit spectrum.

We postpone discussion of the 340 K spectrum in Figure 3A and turn to the PBLG-d_1 spectra shown in Figure 4A. Spectra

(45) Woessner, D. E. *J. Chem. Phys.* **1962**, *36*, 1.
(46) Rananavare, S. Ph.D. Thesis, University of Missouri, St. Louis, 1983, p 263.

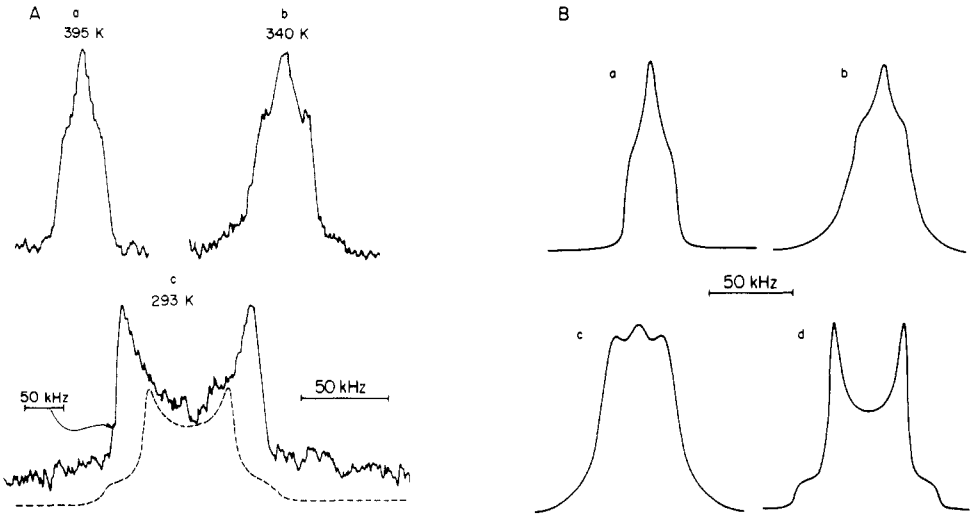

Figure 4. (A) Experimental ^2H NMR spectrum obtained from a powder sample of PBLG-d_1 at the temperatures indicated. The dashed spectrum is identical with spectrum d of part B. (Note the different scale for the full-line spectrum in spectrum c of part A only.) (B) Three-site biased jump model with occupational probabilities in ratios of 1:1:2. Tilt angle between jump axis and the principal axis of the quadrupole tensor is 70.53°. Inhomogeneous line width is 4% of Q_0. Q_0 = 50 kHz. (a) Jump rate = 1.25×10^7 s^{-1}; (b) linear combination of spectra a and c in a ratio of 3:1; (c) jump rate = 3.75×10^3 s^{-1}; (d) jump rate = 0.0 s^{-1}.

a and b are asymmetric powder patterns with[44] $\eta \approx 1$, obtained as a result of partial motional averaging. In the most general terms, such a spectrum is generated by deuterium atoms engaged in nonuniform reorientation about a unique diffusion axis. We have previously discussed flips about the para axis of the benzene ring. This, however, is not being sensed by the deuterium atom of PBLG-d_1, which is located on the jump axis.

Consider now the bond adjacent to the C^ζ–C^η bond, viz., the O^ϵ–C^ζ bond (Figure 1). By postulating a gradual onset of rotational isomerization about successive bonds in the PBLG side chain upon heating, one would naturally inquire about reorientations about the O^ϵ–C^ζ bond. In adopting the dynamic model for our calculations, we were guided by conformational energy computations of the structure of α-helical poly(γ-benzyl L-aspartate) (G. Némethy and H. A. Scheraga, unpublished results), which are the most relevant data available at present to serve as a prototype for this position of the PBLG side chain. The analysis of 24 minimum-energy conformations of the side chain, differing in energy by less than 4.8 kcal/mol, led to a typical pattern of a three-minimum potential about the O^ϵ–C^ζ bond, with one of the three minima considerably deeper than the other two.

In Figure 4B, we show a series of spectra simulated by using a biased three-site jump model for the reorientation around the O^ϵ–C^ζ bond.[47] The occupation probability ratios for the three sites were fixed as 1:1:2, and the jump rates considered were 0.0 s^{-1} (very slow) in Figure 4B, spectrum d, 3.75×10^3 s^{-1} (intermediate) in Figure 4B, spectrum c, and 1.25×10^7 (very fast) in Figure 4B, spectrum a. The experimental spectra obtained at 340 and 395 K both pertain to the high-temperature phase; we interpret the difference in the spectra in terms of temperature-induced differences in dynamic rates. Thus, with the model outlined above, we could reproduce the 395 K spectrum assuming a very fast jump rate (1.25×10^7 s^{-1}), and an intrinsic line width of approximately 4% of the quadrupole interaction. The calculated best fit spectrum is shown in Figure 4B, spectrum a; it corresponds closely to Figure 4A, spectrum a. The 340 K spectrum could not be reproduced with a unique jump rate. It is likely that there is a dynamic distribution, similar to the conformational distribution arising from a number of side-chain structures of comparable energy. We have simulated the 340 K spectrum with two discrete jump rates, namely 1.25×10^7 and 3.75×10^3 s^{-1}, taking 75% of the former and 25% of the latter. We obtained Figure 4B, spectrum b, which may be compared with Figure 4A, spectrum b. The fit is quite satisfactory.

The room temperature spectrum shown in Figure 4A, spectrum c pertains to the low-temperature phase. The spectrum of Figure 4B, spectrum d was obtained by assuming that the three-site jumps described above are frozen out. We have reproduced this spectrum in Figure 4A, spectrum c, where it is shown by the dashed line superimposed on the experimental spectrum obtained at 293 K. It is quite obvious that the latter is approximately twice as broad as the spectrum predicted with the model outlined above. We do, therefore, encounter additional motional averaging, which we first attempted to interpret in terms of a rapid three-site jump process about the C^δ–O^ϵ bond. That would indeed reduce the rigid-limit splitting of roughly 120 kHz between the perpendicular peaks to about 44 kHz, very close to the experimental value of 39 kHz observed at 293 K. Yet, the conformational energy calculations on the benzyl aspartate analogue showed that the potential energy profile about the C^δ–O^ϵ bond has a two-minimum pattern that would generate an asymmetric partially averaged ^2H NMR powder spectrum, in disagreement with the axial powder spectrum observed experimentally. Hence, we conclude that the extra 3-fold reduction in spectral width is brought about by a combined mode of several coupled internal bond isomerizations which, on the whole, act as an axially symmetric averaging process.

We now return to the interpretation of the two-phase spectra of PBLG (d_1 and d_7). We draw upon the close analogy between the liquid crystalline phase formed by the PBLG polymers with halogenic solvents and the phospholipid(lecithin)/water-based liquid crystals. Both systems form hexagonally closed packed structures at lower solvent concentrations.[48]

It is well-known that ends of the phospholipid chains are more flexible and fluid than those near the head groups.[48] A similar model can be envisaged for the ends of the backbone structure of the PBLG helix, which would also enhance the flexibility and fluidity of the associated side chains. As the temperature is raised, one would expect that flexibility and fluidity increase progressively toward the center of the helix. We could then interpret the observed continuous increase in the mobile fraction of benzene rings with increase in temperature as being due to the increase in the fraction of the helical side chains becoming flexible and fluid.

The high-temperature-phase 340 K spectrum of PBLG-d_7 is shown in Figure 3A. The line is quite narrow and isotropic in nature, indicating that the deuterium nuclei are probably experiencing several internal motions that result in overall isotropic averaging. It should be noted that, in spite of salient differences in line shape, the 340 K spectra of PBLG-d_7 (Figure 3) and

(47) Flory, P. J. *Statistical Mechanics of Chain Molecules*; Interscience: New York, 1969; Chapter V.

(48) Chapman, D. *Q. Rev. Biophys.* **1975**, *8*, 185.

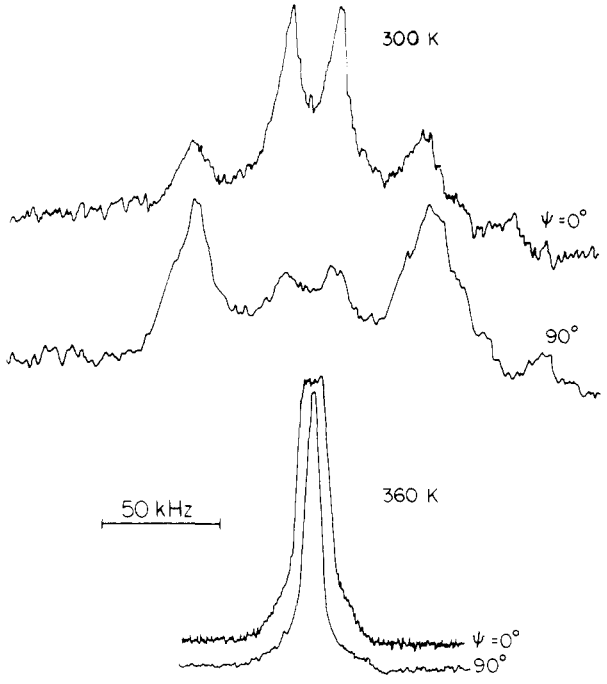

Figure 5. Experimental ^{2}H NMR spectra at 300 and 360 K, obtained from oriented films of PBLG-d_7 prepared as described under Experimental Section; ψ denotes the angle between the external magnetic field and the optical axis of the films (i.e., the uniformly aligned PBLG-d_7 helix axis).

PBLG-d_1 (Figure 4) have comparable widths. Although an NMR spectrum that is isotropic in appearance contains relatively little information about dynamics, we shall consider the 340 K PBLG-d_7 spectrum in light of our interpretation of the 340 K PBLG-d_1 spectrum (see below). Differences in line shape are correlated with the inferior resolution of the former that arises because the spectrum is generated by a multiply labeled (PBLG-d_7) molecule.

More detailed information on the orientation of the benzyl groups in the side chain is obtained from experiments performed on oriented films of PBLG-d_7. ^{2}H NMR spectra obtained at 300 K and 360 K for the external magnetic field parallel ($\psi = 0°$) and perpendicular ($\psi = 90°$) to the PBLG helices are shown in Figure 5.

The 300 K spectra in Figure 5 show two superimposed doublets of unequal intensities that have a pronounced orientation dependence. We associate the stronger doublets with the ortho and meta deuterons on the benzene ring, and we expect, on the basis of our previous discussion, that the benzene ring is engaged in 180° ring flips (cf. Figure 3A). Qualitatively, the observed orientation dependence indicates that the planes of the benzene rings are preferably oriented longitudinally; i.e., their para axis is aligned close to being parallel to the helix axis. The weaker lines in the $\psi = 0°$ spectrum are probably due to methylene deuterons which are immobile. However, it is difficult to rationalize these spectra except in terms of imperfect alignment of the benzene rings (and/or their jump axes) along the helix axis. This distributive nature of the side-chain orientation will cause a severe decrease in the signal-to-noise ratio of the immobile para and methylene deuterons of the amorphous polymer fraction, and only extreme orientations (i.e., those with the principal magnetic axis parallel or perpendicular to the external magnetic field) will generate detectable absorption signals at the position of the weak doublets mentioned above. Additional intensity at those positions may be contributed by a crystalline polymer fraction with crystallites distributed at random in space.

We proceed with a more quantitative analysis of the 300 K spectra in Figure 5. An earlier theoretical calculation[49] indicated

(49) Yan, J. F.; Vanderkooi, G.; Scheraga, H. A. *J. Chem. Phys.* **1968**, *49*, 2713.

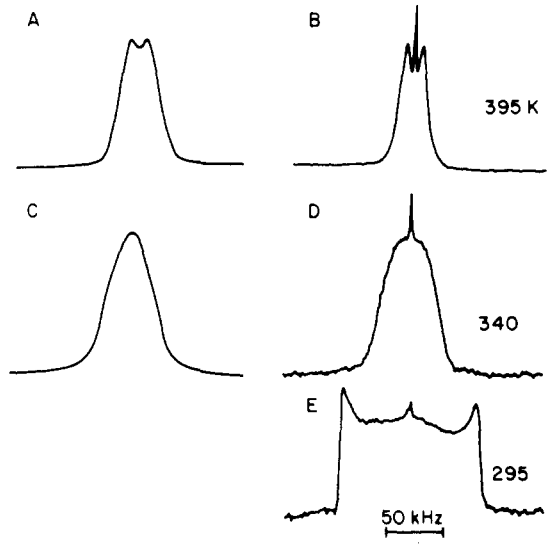

Figure 6. Experimental ^{2}H NMR spectra (B, D, E) obtained from a polycrystalline powder sample of PBLG deuteriated at the γ-carbon position at temperatures indicated in the figure and calculated spectra (A, C) for three-site biased jumps about the C^β–C^γ bond with occupational probabilities in ratios of 0.37:0.37:0.26. The tilt angle between the jump axis and the principal axis of the quadrupole tensor is 70.53°, and orientation-independent intrinsic line widths are on the order of 4% of the quadrupole tensor. The jump rate corresponding to 395 K was 1.25×10^7 s^{-1} (A) and that corresponding to 340 K was 3.2×10^4 s^{-1} (C).

that the para axes of the benzene residues are more likely to be parallel, rather than perpendicular, to the helix axis. It did not, however, specify the exact tilt of the para axis relative to the helix orientation and whether the angle of the tilt is unique. With deuterium labels attached at specific positions on the side chain of an oriented film sample, ^{2}H NMR can provide information, in an unambiguous way, about the relative orientation of the chemical bonds involving the ^{2}H labels. To illustrate the potential inherent in the deuterium NMR experiment to determine molecular geometry, we have considered in the Appendix several extreme orientations of the benzyl residue for which we have calculated the ^{2}H NMR spectra. Comparison of the simulated spectra shown in the Appendix (Figure 14c,d) with the experimental spectra in Figure 5 obtained at 300 K shows that our results corroborate the predictions of ref 49, by indicating that the (predicted lower energy) "longitudinal" model (Figure 4 of ref 49) rather than the "transverse" model (Figure 3 of ref 49) is more realistic.

The analysis of the spectra at 360 K (in Figure 5) is complicated by poor spectral resolution and the effects of multiple reorientations about the intersegmental bonds connecting CD_2–C_6D_5 segments to the polymer backbone. Presumably, the motions of the polymer backbone would also affect the spectra. The spectral width at 90° orientation indicates that all deuterons experience a fast motion. If one chooses to assign a unique diffusion axis, a guess of roughly the magic angle (54.7°) with respect to the external magnetic field seems appropriate. Knowing that the time-averaged spectral widths for all deuterons are between 30 and 40 kHz (see Figure 5, 360 K spectrum), the 0° spectrum would be consistent with a 35° tilt of the diffusion axes with respect to the external magnetic field, in agreement with the guess for the 90° orientation (i.e., 90° − 55° = 35°). Although the NMR measurements, indicating onset of mobility with increasing temperature, cannot entirely exclude the possibility of helix melting (in a helix–coil transition), it is unlikely that such a transition occurs, because it would lead to a loss of the orientational dependence of the PBLG films.

2. PBLG Labeled at the γ-Carbon of the Glutamic Acid Residue: PBLG-d_2 (γ). ^{2}H NMR spectra of PBLG-d_2(γ) are shown in Figure 6. (The sharp liquidlike line centered at the Larmor frequency probably arises from a mobile low-molecular-weight impurity.) The axially symmetric powder pattern, with a splitting of approximately 120 kHz [$\approx(3/4)Q_0$] between the

TABLE I: Low-Energy Conformations[a] of the Uncharged Glutamic Acid Side Chain in α-Helical Uncharged Poly(glutamic acid)[b]

side-chain[c] rotameric state[d]				relative energy,[e]
χ^1	χ^2	χ^3	χ^4	ΔE, kcal/mol
g^-	t	n	t	0.00
g^-	t	p	t	0.34
t	t	p	t	0.66
t	t	n	t	0.69
t	g^+	p	t	0.71
t	g^+	n	t	0.88
g^-	g^-	p	t	1.49
g^-	g^-	n	t	1.56
t	g^-	n	t	1.60
t	g^-	p	t	1.94
g^-	g^+	n	t	2.50
g^-	g^+	p	t	2.81

[a] Computed with the Empirical Conformational Energy Program for Peptides (ECEPP/2) algorithm,[50,51] for CH_3CO-Ala_3-Glu_{10}-Ala_3-$NHCH_3$, where the Ala residues were included to avoid end effects. [b] The backbone of the polypeptide was fixed in a regular α-helical conformation, in which $(\phi, \psi, \omega) = (-68.1°, -38.3°, 180°)$ for each residue.[53] Energy minimization was carried out with respect to the side-chain dihedral angles χ^1, χ^2, χ^3, and χ^4 of each side chain. In each initial conformation (prior to energy minimization), the dihedral angles of all side chains were identical. They were taken from the minimum-energy conformations of a single uncharged glutamyl residue incorporated in a poly(L-alanine) α-helix.[52] Each dihedral angle was allowed to vary independently during energy minimization. [c] The symbols χ^1, χ^2, χ^3, and χ^4 denote the dihedral angles for rotations about the C^α–C^β, C^β–C^γ, C^γ–C^δ, and C^δ–O^ϵ bonds, respectively.[55] [d] Ranges of dihedral angles for each rotameric state are denoted as follows. For bonds with 3-fold rotation, t for $120° \le \chi \le 180°$ and $-180° \le \chi \le -120°$, g^+ for $0° \le \chi \le 120°$, and g^- for $-120° \le \chi \le 0°$. For the 2-fold rotation about the C^γ–C^δ bond, p and n denote $0° < \chi^3 \le 180°$ and $-180° < \chi^3 \le 0°$, respectively. [e] Expressed per glutamyl side chain and relative to the energy of the lowest energy conformation shown (line 1); i.e., $\Delta E = (E - E_0)/10$, where $E_0 = -162.48$ kcal/mol is the total computed energy of the molecule with the conformation shown in line 1 of the table.

main peaks, recorded at 295 K, indicates that these deuterium atoms are static on the ^2H NMR time scale up to this temperature. Since similar results were obtained with PBLG-d_1 (see Figure 4A), we conclude that the PBLG side chain extending from the γ-carbon to the para axis of the benzene ring does not experience any dynamic process other than rapid ring flips below room temperature (see above).

PBLG undergoes a phase transition at about 330 K (see discussion below). Our objective is to interpret the PBLG-$d_2(\gamma)$ dynamic line shape observed in the higher temperature phase in terms of molecular parameters. Yet, meaningful deductions can be made only with some prior knowledge of the static conformation at the site of the magnetic nucleus. No detailed conformational analysis is available for PBLG that would provide structural information about the lowest energy side-chain conformations. A comparative analysis of poly(glutamic acid), PBLG, and several derivatives of PBLG with substitutions on the benzene ring has indicated that the dihedral angles and relative energies of the favored side-chain conformations are similar for these polypeptides.[49] Therefore, for the γ-position in the side chain, it is possible to use the results of conformational energy computations[50,51] on glutamic acid residues inserted in a poly(L-alanine) α-helix,[52] in order to suggest preferred conformations for PBLG side chains in an α-helix. When glutamic acid is incorporated in a regular α-helix,[53] only two low-energy rotameric states[54] of the C^α–C^β bond (described by the dihedral angle[55] χ^1) exist, viz., the states t and g^-, while all three rotameric states t, g^-, and g^+ can occur for the C^β–C^γ bond, with a slight preference for the t state[52] (Table I). Thus, several rotameric states are of low energy for the side chains in poly(glutamic acid) and, by implication, for PBLG. Even without performing detailed line shape calculations, it is quite obvious that the adoption of a model for PBLG that assumes that the dominant dynamic process affecting the deuterons at the γ-position is a combination of rotational isomerization about the C^α–C^β and the C^β–C^γ bonds would be a reasonable starting point.

We could simulate the ^2H NMR spectra obtained at 340 and 395 K from the γ-labeled PBLG sample with a three-site model for the motion about the C^β–C^γ bond. Relative populations of 0.37:0.37:0.26 were assumed, and the tilt angle was taken equal to 70.53°. The best calculated spectra are shown in parts A and C of Figure 6 (displayed next to the corresponding experimental traces), obtained with jump rates of 1.25×10^7 and 3.2×10^4 s^{-1}, respectively. Clearly, for 340 K the fit is satisfactory, indicating that the jump rate at that temperature is 3.2×10^4 s^{-1}. Although the shape of the experimental spectrum obtained at 395 K is reproduced, the overall width is overestimated by the theoretical model. This discrepancy can be accounted for by assuming additional rapid temperature-dependent librations (or a combined mode of coupled internal bond isomerization acting, on the whole, as an axially symmetric averaging mechanism) which are quite effective at 395 K and marginal in their spectral consequences at 340 K.

It may be noticed that, at about 395 K, all the spin-labels, regardless of their position on the side chain, have comparable NMR spectral width. Our analysis of the solid-phase spectra at 295 K from the aligned PBLG-d_7 films quite clearly demonstrated that the orientation of the benzene ring para axis is parallel to the helix axis. The situation is not so obvious, however, regarding the orientation of the side chains in the high-temperature phase. This is due to the onset of rapid (on the deuterium NMR time scale) multiple reorientations around the intersegmental bonds at the phase transition that prevent us from studying the orientation-dependent slow motional spectra. The interpretation of spin-label dynamics, in terms of two- or three-site jumps, is rather dangerous because the actual number of sites involved in the problem is not simply related to the rotational symmetry of the potential around the adjacent bond. To illustrate this point, consider the high-temperature spectra of the γ-deuterons and that of the para deuteron on the aromatic ring. If the motion of the intermediate bonds were completely independent (i.e., uncorrelated), one would have predicted a spectrum with an order of magnitude smaller spectral width for the para deuteron. This is quite clearly not the case. Also, the fact that we observe an axially asymmetric line shape for the para deuteron indicates that the motional rate for the reorientation around the O^ϵ–C^ζ bond is at least an order of magnitude faster than any other (overall) axially symmetric jump process in the side chain.

At this point, we would like to comment on the 340 K phase transition observed in the PBLG system. NMR data below 340 K rule out the presence of any large-amplitude motions of the side chains except for the benzene ring flips. However, our conformational analysis for an isolated α-helix indicates that at least 30–40 conformational states have comparable stabilization energies and sufficiently low activation energy barriers for transitions among them. This implies that at room temperature the effects of interconversions should motionally narrow the deuterium NMR spectra of the spin-labels employed. The physical origin of this discrepancy is clear if one recognizes that the conformational analysis is carried out for a single α-helix. The effects of the neighboring helices, arranged in a hexagonal lattice surrounding the helix under consideration, were not included in the calculations. If steric interactions relevant in the crystalline lattice were considered, it is clear that there exist severe additional restrictions,

(50) Momany, F. A.; McGuire, R. F.; Burgess, A. W.; Scheraga, H. A. *J. Phys. Chem.* **1975**, *79*, 2361.
(51) Némethy, G.; Pottle, M. S.; Scheraga, H. A. *J. Phys. Chem.* **1983**, *87*, 1883.
(52) Piela, L.; Némethy, G.; Scheraga, H. A. *Biopolymers* **1987**, *26*, 1273.
(53) Chou, K. C.; Némethy, G.; Scheraga, H. A. *J. Am. Chem. Soc.* **1984**, *106*, 3161.
(54) Vásquez, M.; Némethy, G.; Scheraga, H. A. *Macromolecules* **1983**, *16*, 1043.
(55) IUPAC–IUB Commission on Biochemical Nomenclature *Biochemistry* **1970**, *9*, 3471.

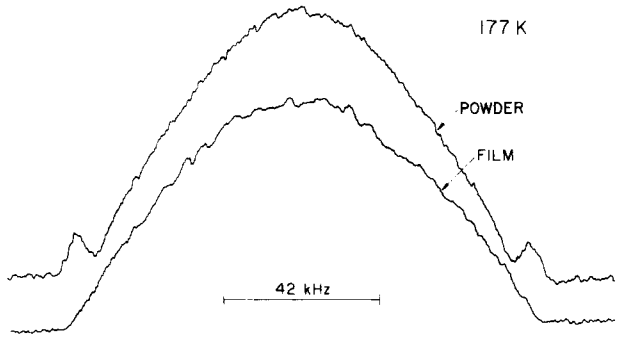

Figure 7. Experimental ^{2}H NMR spectra obtained from an oriented film of PELG-d_2 (bottom) and from a precipitated powder sample at 177 K. (Note that the spectra from the oriented film are independent of the direction of the film axis relative to the magnetic field.)

due to neighboring molecules, on the calculated side-chain conformations, as well as on the rates of interconversions among them.

With this rationale in mind, the analysis of the high-temperature-phase deuteron NMR spectra implies that, at the phase transition, the extent of the nearest-neighbor interactions is dramatically reduced. One may then envision the phase transition as two-dimensional melting of the helix array (similar to the gel–lamellar phase transition found in lipids). In the high-temperature phase, the comparison between the conformational populations derived from deuteron NMR line shape simulations and the conformational analysis is better justified. The results compare favorably, within the limitations of each technique.

Below the phase transition, the γ-deuterium atoms are static on the ^{2}H NMR time scale, as mentioned previously.

B. Poly(γ-ethyl L-glutamate) (PELG) Labeled at the Ester Positions: PELG-d_3 and PELG-d_2. PELG polymers were labeled selectively at the methyl and methylene positions, respectively, of the ester moiety. With these selectively labeled species, we could obtain fairly well-defined morphologies [i.e., magnetically oriented paracrystalline films (and precipitated powders) with a small degree of crystallinity] and information about side-chain orientation and segmental mobility. In Figure 7, we show ^{2}H NMR spectra from a powder sample (upper spectrum) and from an oriented film of PELG-d_2, both recorded at 177 K. It is clear that the outer sharp peaks, with a splitting of approximately 120 kHz, are present only in the powder spectrum. As discussed previously, a typical axial rigid-limit powder spectrum of an aliphatic deuteron has the intense "perpendicular" peaks separated by roughly 120 kHz; the weaker parallel shoulders, separated by 240 kHz, are often lost in the background noise. With PBLG-d_7 we attributed the excessive intensity of the perpendicular peaks to the combined effect of immobile labels pertaining to the amorphous and the crystalline morphologies. With PELG-d_2, the amorphous component obviously does not contain immobile deuterium atoms. Therefore, the rigid component in the powder spectrum is due solely to the presence of crystallites from the precipitation procedure, whereas the oriented film from the casting procedure exhibits a single-component line shape generated by a purely amorphous polymer; it is a dynamic spectrum, reflecting partial motional averaging due to anisotropic internal motions.

A similar conclusion emerges from the powder spectra of PELG-d_3 shown in Figure 8. Each line shape is dominated by a dynamic spectrum, contributing primarily at the center and associated with the amorphous polymer fraction, and an axial powder spectrum, with "perpendicular" peaks separated by approximately 43 kHz, associated with the crystalline component. Our interpretation of the PELG-d_3 powder spectrum is analogous to that of the PELG-d_2 powder spectrum, except for rapid methyl reorientation experienced by the methyl deuterons. Thus, the 120-kHz perpendicular peak separation observed with PELG-d_2 is reduced to 120 $(^1/_2)(3\cos^2 71° - 1) \approx 43$ kHz with PELG-d_3 (71° being the valence angle between the symmetry axis of the methyl group and the C–D bonds). Similar to PELG-d_2, spectra obtained from oriented films are free of crystallites, as illustrated in Figure 9, where we present a series of temperature-dependent

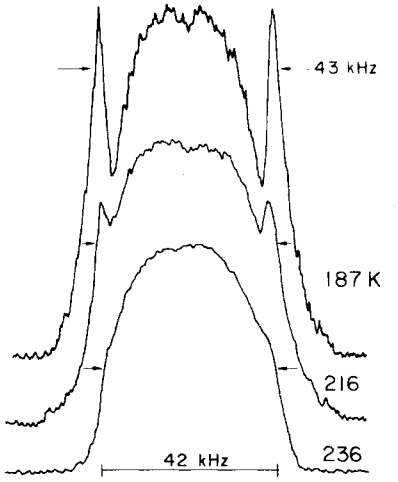

Figure 8. Experimental ^{2}H NMR spectra from a precipitated powder of PELG-d_3 at various temperatures.

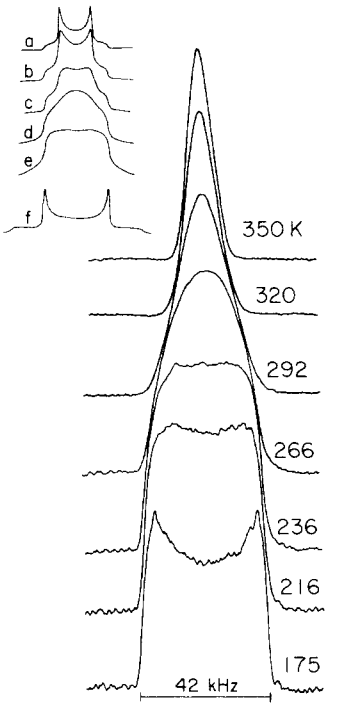

Figure 9. Experimental ^{2}H NMR spectra from an oriented film of PELG-d_2 at the temperatures indicated. (The spectra are independent of the direction of the film axis relative to the magnetic field.) (Inset) Spectra calculated by assuming discrete 120° jumps between three equivalent sites about a diffusion axis tilted at 90° relative to the principal axis of an axial quadrupole tensor (details on the calculation are given in the Appendix of ref 56). A natural line width on the order of several percent of the quadrupole coupling constant was used, and the jump rates expressed in units of the quadrupole coupling constant are as follows: (a) 1.2×10^3, (b) 16, (c) 4.7, (d) 1.5, (e) 0.6, and (f) 1.2×10^{-3}.

spectra from PELG-d_3 films. Comparison with Figure 8 indicates that the 216 and 236 K spectra in Figure 9 can be obtained from the corresponding line shapes in Figure 8 by subtracting the rigid component.

It should be noted that we did not specify the orientation of the film with respect to the external magnetic field while discussing the spectra of Figures 7 and 9. This is unnecessary, given the unexpected observation that, with PELG films, the ^{2}H NMR spectrum is independent of film orientation, in contrast to the PBLG-d_7 films. Since the existence of uniform, parallel orientation of the helices has been established by an X-ray diffraction examination, we conclude that, in spite of helix alignment, the PELG side-chain orientations are distributed randomly, i.e., there is no discrete side-chain structure, as evidenced by the NMR spectra of the deuterons in the ester group.

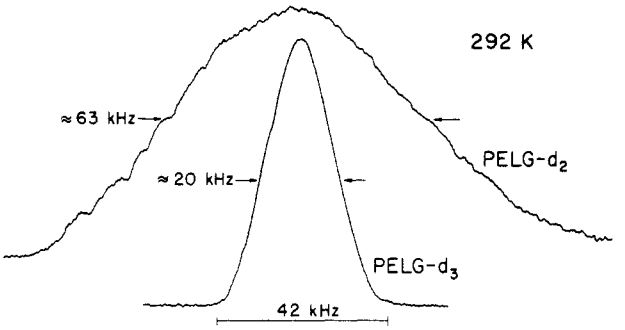

Figure 10. Experimental ^2H NMR spectra from oriented films of PELG-d_2 (top) and PELG-d_3 at ambient temperature.

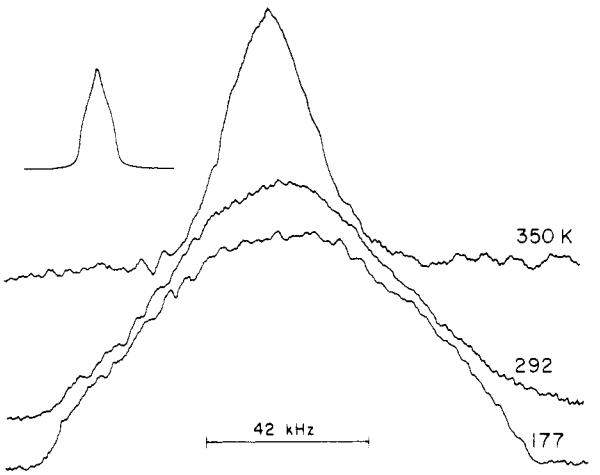

Figure 11. Experimental ^2H NMR spectra from an oriented film of PELG-d_2 at the temperature indicated. The inset shows the shape of the computed curve (not to scale) for a three-site biased-jump model with occupational probabilities in ratios 1:1:2. The tilt angle between jump axis and Q_{zz} tensor is 70.53°. The inhomogeneous line width is 4% of Q_0. Jump rate = 1.25×10^5 s^{-1}.

Figure 10 shows again that the methyl and the methylene deuterons exhibit the same overall spectral features, except for reduction of the methyl spectra due to internal reorientation. In Figure 11, we present spectra obtained with PELG-d_2 films at various temperatures. Unfortunately, the spectral resolution is low; in addition, the line shape is probably distorted because of the length of the 90° pulse. We could not decrease this instrumental parameter below 7.4 μs in this particular experiment; to check the extent to which this affects our spectra, we lowered the temperature to 150 K, where the line shape is close to a true rigid-limit pattern, and found that the central portion of the axial powder spectrum is typically of greater amplitude due to the large pulse length.[19]

In summary, the line shapes of the spectra of only Figure 9 warrant a quantitative analysis. We reiterate that the 175 K spectrum is an axially symmetric powder pattern with roughly 43 kHz between the main peaks showing an onset of slow motional effects, consistent with a collection of rapidly rotating methyl groups having their C_3 axes distributed at random in space. Further spectral averaging observed upon heating is then associated with additional motional processes involving the methyl deuterons.

The trends reflected in the evolution of the spectra between 177 and 266 K are typical of discrete jumps between three equivalent sites about a diffusion axis perpendicular to the C–CD_3 bond, with gradually increasing jump rates. This is quite obvious if we compare the corresponding experimental line shapes in Figure 9, with the calculated spectra shown in the inset of Figure 9, obtained[56] with a model of C_{3v} jumps about a perpendicular diffusion axis.

(56) Meirovitch, E.; Belsky, I.; Vega, S. *J. Phys. Chem.* **1984**, *88*, 1522.

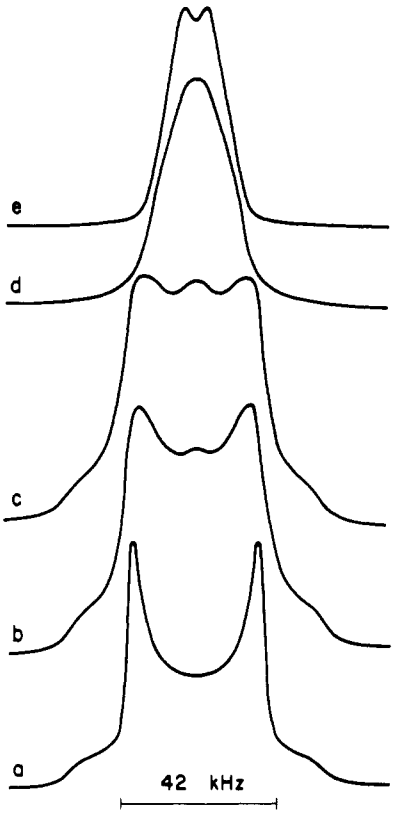

Figure 12. Three-site biased-jump model with occupational probabilities in ratios of 0.37:0.37:0.26. The tilt angle between the jump axis and the principal axis of the quadrupole tensor is 70.53°. Orientation-independent inhomogeneous line widths are 4% of Q_0. (a) Jump rate = 0.0 s^{-1}; (b) jump rate = 1.25×10^3 s^{-1}; (c) a mixture of spectra with a jump rate of 1.25×10^4 and a jump rate of 1.25×10^3 in a ratio of 0.15:0.85; (d) jump rate = 3.2×10^4 s^{-1}; (e) jump rate = 1.25×10^7 s^{-1}.

The similarity of the lower temperature experimental spectra and the corresponding theoretical inset spectra appears to indicate that the model used in the calculations, with a 90° tilt between the diffusion axis and the C–CD_3 bonds, is a reasonable one. We estimate that the error in this orientation of the diffusion axis does not exceed ±10°. Consequently, the experimental line shapes between 175 and 266 K could not be reproduced with a tilt of 71°, which would correspond to jumps about the O^ϵ–C^ζ bond. In fact, none of the chemical bonds of the side chain in the vicinity of the C^ζ–CD_3 bond are perpendicular to the O^ϵ–C^ζ bond in any low-energy conformation.

Alternatively, the experimental spectra in Figure 9 can be reproduced with a biased three-site jump motion about the C^δ–O^ϵ bond (i.e., a 71° tilt between the jump axis and the principal magnetic axis). We depict such an attempt in Figure 12, to be compared with Figure 9. Although the majority of the spectra in the series of Figure 9 can be reproduced satisfactorily with unique jump rates increasing from 0.0 to 1.25×10^7 s^{-1} (see legend of Figure 12), in some cases the fit is improved considerably by admixing spectra calculated with different jump rates (see spectrum c of Figure 12).

The dramatic temperature-dependent spectral effects exhibited by the methyl deuterons, but not by the methylene deuterons over the same temperature range, can be attributed to the different time scale needed to average out the methyl and methylene deuteron quadrupolar interactions. Recall that for a simple spectrum of two Lorentzian lines, separated by frequency differences $\Delta\omega$ and which coalesce to a single line by a jump process (described by a jump rate $1/\tau$), motional effects are most dramatic at $\tau\Delta\omega \approx 1$. Similar considerations for the motion of the methyl and methylene group would imply that a motional process affecting dramatically the 43-kHz methyl splitting would have a rate that is about a factor of 3 slower than required to affect the methylene deuterons dramatically.

The correspondence between experimental and calculated spectra (cf. Figure 9) is degraded close to room temperature, due, presumably, to the onset of additional motions which average out the quadrupolar interaction efficiently and uniformly. This is too complex a situation to warrant detailed interpretation, since all the anisotropic features of the NMR line shape that would be needed are "washed out" by the averaging process. It is possible that the nearby environment of the methyl group could be mapped out by observing other magnetic nuclei, thereby clarifying the situation to some extent. We tried to simulate only the high-temperature (350 K) spectrum in Figure 11 for the methylene deuterons, using the same model as in Figure 9a,b but with a jump rate of 1.25×10^5 s^{-1}, and obtained the spectrum shown in the inset of Figure 11. Thus, the apparent ability of this model to predict the spectra for the two different systems is indicative of the similarity of the intersegmental potentials about the O^{ϵ}–C^{ζ} bond in both PBLG and PELG.

It is, however, appropriate to comment on the abrupt change in the efficiency of the averaging process, which increases dramatically above room temperature as illustrated by the spectra of both Figure 9 and Figure 11. These observations are suggestive of a phase transition, similar to that observed with the PBLG polymer. The structural collapse of the PELG-d_3 spectra at about 266 K indicates that, even below the phase transition, motions other than the 3-fold jumps affect the deuterium atoms.

C. Conformational Mobility of PBLG Side Chains. We compare below our NMR results and the structural information provided by theoretical conformational energy calculations of the ordered structures of poly(amino acids) and their derivatives.[49,52] For PBLG in a right-handed α-helix, Yan et al.[49] showed that a longitudinal conformation, with the side chains lying approximately parallel to the helix axis, is preferred over the transverse conformation, in which the side chains lie approximately perpendicularly to the helix axis. A more recent computational study[52] of glutamic acid in an α-helix showed, however, that these two conformations are comparable in energy (cf. the t and g$^-$ rotameric states for χ^1 in Table I, corresponding to longitudinal and transverse orientations, respectively). From dipole moment measurements, Erenrich and Scheraga[57] concluded that there is a random distribution of the PBLG side chains, in agreement with the conformational energy computations (ref 52 and Table I). This, however, is based on measurements in dilute solution and is, therefore, not quite relevant to the results of our solid-state study. On the other hand, Samulski[58] found a nonrandom side-chain orientation in a liquid crystalline phase,[59-61] which may be more relevant to a solid material.

The results obtained with the oriented PBLG-d_7 films are in accord with the structure reported by Yan et al.[49] in the sense that the side chains take on a longitudinal conformation, having the para axis of the ring aligned close to the helix axis. The NMR experiment is definitely sensitive to the spatial distribution of the benzene rings. Further experiments on oriented PBLG films are very likely to lead to the elucidation of the functional form of the side-chain distribution about the helix axis.

The conformational analysis of glutamic acid in an α-helix[52] indicates that there are two preferred positions for the C^{γ} atom of the glutamyl side chain, corresponding to rotameric states t and g$^-$ of the C^{α}–C^{β} bond (Table I), with comparable energies. There are no analogous data available for PBLG. While it is possible that the presence of the γ-benzyl substitution modifies the relative energies of various glutamyl side-chain conformations somewhat, it is not likely that the position of the C^{γ} atoms (determined by the dihedral angle χ^1) would be altered noticeably by this substitution, because their position (and the preference for the t and g$^-$ rotamers over the g$^+$ rotamer) are determined

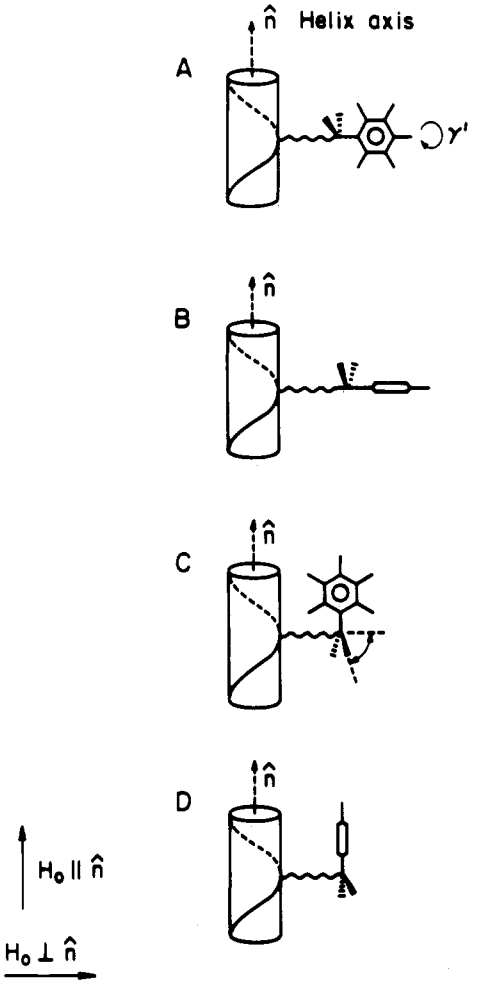

Figure 13. Models considered for various directions of alignment of CD_2–C_6D_5 segments, in relation to helix axis ($\hat{n}$) and to external magnetic field, H_0, as specified in the Appendix. Only the two extreme relative orientations (viz., parallel and perpendicular) of H_0 and $\hat{n}$ were considered. The dihedral angle for rotation of the benzene ring about the para axis is defined as $\gamma' = 0°$ and $\gamma' = 90°$ for models A and B, respectively.

primarily by the interaction of the $C^{\gamma}H_2$ group with the polypeptide backbone.[62] Therefore, it is reasonable to assume that PBLG and poly(glutamic acid) in the α-helical form have similar side-chain conformations at the γ-position. As detailed in the text, ^{2}H NMR results are consistent with these theoretical calculations. The potential of ^{2}H NMR for providing information about the structure and dynamics of biopolymers is borne out by these results.

D. Future Possibilities. On the basis of this work we can suggest new experiments and procedures that we believe would improve the understanding of the structure and dynamics of polymers by NMR. These include (a) the study of well-aligned liquid crystalline phases;[59-61] (b) the application to NMR[63] of a new two-dimensional "T_2-type" experiment, originally developed for ESR,[64] that greatly increases the resolution and sensitivity to dynamics when dealing with inhomogeneously broadened lines; (c) the use of other appropriate spin relaxation methods;[65,66] and (d) the application of double-quantum ^{2}H spectroscopy[3] to cancel the effects of the quadrupole interaction and to focus on the different chemical shifts of the deuterons in chemically different positions.[67]

(57) Erenrich, E. H.; Scheraga, H. A. *Macromolecules* **1972**, *5*, 746.
(58) Samulski, E. T. *J. Phys., Colloq.* **1979**, Ser. C3, *40*, 471.
(59) Yamazaki, T.; Toriumi, H.; Abe, A., private communication.
(60) Czarniecka, K.; Samulski, E. T. *Mol. Cryst. Liq. Cryst.* **1981**, *63*, 205.
(61) Toriumi, H.; Yamazaki, T.; Abe, A.; Samulski, E. T. *Liq. Cryst.* **1986**, *1*, 87.
(62) Benedetti, E.; Morelli, G.; Némethy, G.; Scheraga, H. A. *Int. J. Pept. Protein Res.* **1983**, *22*, 1.
(63) Rananavare, S.; Freed, J. H., to be published.
(64) Millhauser, G. L.; Freed, J. H. *J. Chem. Phys.* **1984**, *81*, 37.
(65) Spiess, H. W. *J. Chem. Phys.* **1980**, *72*, 6755.
(66) Schwartz, L. J.; Millhauser, G. L.; Freed, J. H. *Chem. Phys. Lett.* **1986**, *127*, 60.

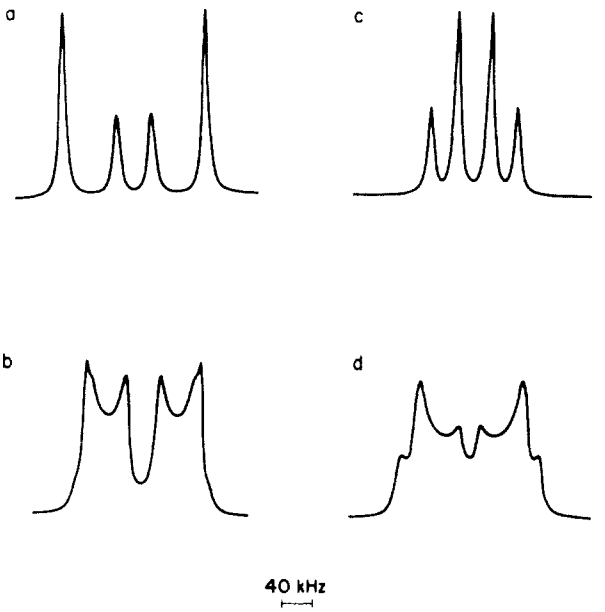

Figure 14. Simulated ^2H NMR spectra for aligned PBLG films. Spectra were simulated by performing orientational averaging, as well as motional averaging (benzene ring flips). The four spectra correspond to the models shown in Figure 13, as follows: (a) model A, for $H_0 \| \hat{n}$; (b) model A, for $H_0 \perp \hat{n}$; (c) models C and D, for $H_0 \| \hat{n}$; (d) models C and D, for $H_0 \perp \hat{n}$. Note that models B and D are two-dimensional powder patterns.

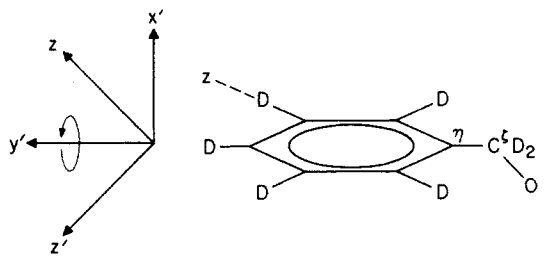

Figure 15. Schematic drawing of the benzyl side chain of PBLG-d_7, illustrating the magnetic z axis, aligned with the ortho and meta deuterons, and a right-handed Cartesian coordinate system for which x' is perpendicular to the plane of the ring, y' is parallel to the C^ζ–C^η axis, and z' lies in the plane of the ring. The z axis is the principal axis of the rigid-limit quadrupole tensor, while x', y', z' is the coordinate frame of the partially averaged quadrupole tensor. For discrete 180° jumps about the C^ζ–C^η axis (curved arrow), the principal values of the partially averaged asymmetric tensor appear along x', y', and z'.

V. Conclusions

(1) We have illustrated the use of ^2H NMR spectroscopy to investigate phase transitions and conformational dynamics of polymers.

(2) We observe a definite phase transition at 330 K in PBLG, which we characterized as side-chain "melting". A similar transition appears to occur in PELG but is less clearly characterized.

(3) In the lower temperature phase of PBLG (below 330 K) the only motion present in side chains is the 180° flipping of benzene rings. One observes a gradual melting of these rings in such a way that, as the temperature is raised (within this phase), the fraction of benzene rings engaged in rapid flipping increases toward 100% near the transition point.

(4) The use of partially aligned samples permitted us to determine the orientation of the benzene rings in the (more rigid) low-temperature phase. In particular, we concluded for PBLG that there is a preferential orientation of the plane of the benzene ring parallel to the helix axis. This is reasonably consistent with theoretical studies of side-chain conformations for the isolated α-helical polypeptides. For PELG, on the other hand, no preferential alignment of the ethyl groups could be detected.

(5) Above the phase transition in PBLG, there is an additional motion about the O^ϵ–C^ζ axis. While more than one model of this motion can fit the data, a successful one that we consider to be reasonable is a three-site biased population model. Again, there are two populations of side chains, viz., rapidly and slowly rotating benzyl groups. The former become predominant as the temperature is raised.

(6) The theoretical calculations of the intersegmental potential for the O^ϵ–C^ζ bond agree with the occupational probabilities for the three conformers that are obtained from the NMR analysis.

Acknowledgment. This work was supported by research grants at the University of Connecticut [NIH-AM-17497 (E.T.S.)] and at Cornell University [NIH-GM-24893 (H.A.S.), NIH-AG-00322 (G.N.), NSF-DMB84-01811 (H.A.S.), NIH-GM-25862 (J.H.F.), and NSF-DMR86-04200 (J.H.F.)]. We thank Dr. K. Nagayama for the sample of PBLG-$d_2(\gamma)$. E.M. acknowledges funds granted by the Minerva Foundation.

Appendix. Analysis of Spectra from Oriented Films

With the methods at hand, we tried to simulate the oriented-film spectra of Figure 5 by considering hypothetical models shown in Figure 13. These models correspond to extreme combinations of the relative orientation of helix axis ($\hat{n}$), magnetic field (H_0), and the rotational axis of the benzene ring. Examples A and B correspond to extreme positions in which the para axis of the benzene ring is oriented normal to the helix axis, while examples C and D correspond to the other extreme orientation, in which the para axis is parallel to the helix axis. We show in Figure 14 simulations computed for rapid flips of benzene rings around the para axis with the geometries shown in Figure 13. The spectra for $H_0 \| \hat{n}$ were simulated by using a Gaussian distribution of the CD_2–C_6D_5 segments centered about the para axis. If the benzene rings are oriented normal to the helix axis (cf. Figure 13A,B), the peak positions due to the ortho and meta deuterons will be at (A) $2\delta_0 P_2$ (cos 30°) = 175 kHz or at (B) $2\delta_0 P_2$ (cos 90°) = −140 kHz [where P_2 (cos θ) ≡ (3 cos^2 θ − 1)/2], both of which are incompatible with experimental observation. However, it should be noted that, since the benzene ring is oriented at an angle γ' (cf. Figure 13A) between these extrema, it is possible to shift the peak positions due to the ortho and meta deuterons into the center of the spectrum (e.g., γ' = 54.5° yields a splitting of 35 kHz). Such an orientation of the benzene ring is clearly not permitted, however, due to the steric hindrance of an ortho deuteron with hydrogens of the adjacent methylene group. A rotation about the O–CD_2 bond that would result in a tilt of 54.5° of the para axis of the benzene ring with respect to the magnetic field will render two methylene deuterons nonequivalent, and the intensity of the peaks at 100 kHz will be drastically reduced. Therefore, models A and B can be eliminated.

A similar process will show that, if the para axes of the rings are oriented parallel to the helix axis (Figure 13C,D), the splittings are in rough agreement with the experimental observations (see Figures 14c,d and 5). However, one cannot distinguish between model C and model D on the basis of the $H_0 \| \hat{n}$ spectrum alone.

The $H_0 \perp \hat{n}$ spectra were simulated by using a two-dimensional powder averaging method, since the x' axis drawn normal to the planes of the benzene rings (Figure 15) is distributed randomly in the plane normal to the helix axis (cf. Figure 14c,d). Models C and D yielded identical 2D powder-averaged spectra, as expected from considering Figure 13C,D. The analysis shows that the intensity in the central part of this spectrum (Figure 14d) is due to one of the extrema in the two-dimensional powder patterns of the methylene deuterons, consistent with the relatively low intensity of the methylene deuterons in this spectral region (cf. Figure 5).

Additionally, we tried to introduce tilting around the O^ϵ–C^ζ bond such that it bends the para axes of rings toward the helix, even beyond the position shown in Figure 13C. The simulations seem to give a better fit for the $H_0 \perp \hat{n}$ spectrum. We found that a tilt of only 10–12° is needed to obtain a fair agreement with the experimental spectrum. However, it should be noted that once

(67) Ref 3, Chapter 6.

a tilt is introduced, models C and D become nonequivalent with respect to powder averaging, and an additional tilt angle is needed to define the plane of the benzene ring. In view of the experimental spectral distortions (cf. Experimental Section), we did not attempt further simulations to pursue this point. Thus, qualitative analysis seems to favor either model C or D, in agreement with ref 49. We note in passing that the g^- state for the γ-position has slightly lower conformational energy than the t state (cf. Table I), thereby favoring the parallel orientation of the para axis with respect to the helix axis.

Molecular Mobility of Poly(methyl methacrylate): A Time-Resolved Electron Spin Resonance Study with Photoexcited Triplet-State Phenazine as a Probe

Soon Sam Kim,* Fun-Dow Tsay, and Amitava Gupta

Applied Sciences and Microgravity Experiments Section, Jet Propulsion Laboratory, California Institute of Technology, Pasadena, California 91109 *(Received: February 3, 1987; In Final Form: May 4, 1987)*

Molecular mobilities of poly(methyl methacrylate) (PMMA) doped with phenazine as a probe were investigated by employing a time-resolved electron spin resonance (ESR) technique.[1] Amplitudes of the transient ESR responses from photoexcited triplet phenazine molecules were monitored immediately after a pulse from an excimer laser (308 nm). The amplitudes were measured at several microwave powers with the probes in PMMA matrices of different average molecular weights. The transient ESR data are found to correlate with the relative molecular mobilities of host matrices as reflected by the differences in their glass transition temperatures. The time scale of motions detected by this method is in the range of 10^{-4}–10^{-6} s.

Introduction

The use of molecular probes for studies of molecular mobilities in polymeric matrices has been well documented. The nitroxide free radical spin-labels and spin-probes have been widely used for the purpose with conventional electron spin resonance applications[2-4] (for faster motions with correlation time $10^{-11} < \tau_2 < 10^{-7}$ s), or with saturation transfer techniques[5] (for slower motions, $10^{-7} < \tau_2 < 10^{-3}$ s). Since then the spin-label or spin-probe methods have been expanded to the use of biradical probes,[3] isotopically enriched nitroxide labels,[6-8] e.g., deuterium or ^{15}N substituted nitroxide free radicals, for certain advantages in probing molecular motions. Recently, the nitroxide labels were studied with instrumental sophistication, e.g., applications of electron nuclear double resonance[9] and electron spin–echo[10] techniques.

Nuclear magnetic resonance spectroscopy was also applied to the study of slow motional modes in solids, e.g., Kuhns and Conradi[11] with their NMR hole-burning technique and Mortimer et al.[12] with their NMR spin–echo method.

As for optical probes, various organic molecules were used as fluorescence[13,14] and phosphorescence[15,16] probes to study molecular mobilities.

TABLE I: Poly(methyl methacrylate) Used in the Experiment

	M_n	M_w/M_n	T_g, °C measd[a]	T_g, °C calcd[b]
PMMA of broad mol wt distribution	209 000	1.83	123	113
	22 000	4.91	108	103
	11 000	9.34	104	94
mol wt standards	100 000	1.10	119	111
	30 000	1.10	116	106

[a] Measured by DSC, at temperature scan rate of 10 °C/min. [b] Calculated by using the parameters of PMMA in ref 31.

As an analogy to the phosphorescent probe used in optical spectroscopy, we used the phenazine molecules in their phosphorescent state as probes and detected by a time-resolved ESR technique to study molecular mobilities in glassy polymers. In this paper, we describe the preliminary results of the time-resolved ESR studies carried out with phenazine probes in poly(methyl methacrylate) (PMMA) matrices.

In a glassy polymer like PMMA at room temperature, the most likely motions of phenazine probes one can expect are from slow tumbling to librational motions. The motions of probes are in turn reflections of those of host polymer matrices, e.g., side chain segmental motions, large-scale main chain motions, etc. The very fact that one can observe ESR spectra from the triplet-state phenazine molecules in PMMA limits that the motions involved are much slower than in liquid state.

It is well-known that the phenazine molecules in their first excited triplet states exhibit optical electron spin polarization.[17] It is also reported that when detected by time-resolved ESR technique,[18] one can observe transient nutations from the triplet-state phenazine molecules. The waveform of transient nutation

(1) Kim, S. S.; Weissman, S. I. *J. Magn. Reson.* **1976**, *24*, 167.
(2) Ranby, B.; Rabek, J. F. *ESR Spectroscopy in Polymer Research*; Springer-Verlag: West Berlin, 1977.
(3) Berliner, L. J. *Spin Labeling, Theory and Applications*; Academic: New York, 1976 and 1979; Vol. I and II.
(4) Dalton, L. R. *EPR and Advanced EPR Studies of Biological Systems*; CRC: Boca Raton, FL, 1985.
(5) Thomas, D. D.; Dalton, L. R.; Hyde, J. S. *J. Chem. Phys.* **1976**, *65*, 3006.
(6) Li, A. S. W.; Hwang, J. S. *J. Phys. Chem.* **1985**, *89*, 2556.
(7) Gaffney, B. J.; Elbrecht, C. H.; Scibilia, J. P. A. *J. Magn. Reson.* **1981**, *44*, 436.
(8) Lee, S.; Shetty, A. *J. Chem. Phys.* **1985**, *83*, 499.
(9) Kotake, Y.; Tomita, Y.; Kuwata, K. *J. Phys. Chem.* **1985**, *89*, 207.
(10) Szajdzinska-Pietek, E.; Maldonado, R.; Kevan, L.; Berr, S. S.; Jones, R. R. M. *J. Phys. Chem.* **1985**, *89*, 1547.
(11) Kuhns, P. L.; Conradi, M. S. *J. Chem. Phys.* **1982**, *77*, 1771.
(12) Mortimer, M.; Oates, G.; Smith, T. B. *Chem. Phys. Lett.* **1985**, *115*, 299.
(13) de Silvestri, S.; Weiner, A. M.; Fujimoto, J. G.; Ippen, E. P. *Chem. Phys. Lett.* **1984**, *112*, 195.
(14) Noel, C.; Laupretre, F.; Friedrich, C.; Leonard, C.; Halary, J. L.; Monnerie, L. *Macromolecules* **1986**, *19*, 201.
(15) Miller, L. J.; North, A. M. *J. Chem. Soc., Faraday Trans. 2*, **1975**, *71*, 1233.
(16) Rutherford, H.; Soutar, I. *J. Polym. Sci., Polym. Phys. Ed.* **1977**, *15*, 2213.
(17) Furrer, R.; Gromer, J.; Kacher, A.; Schwoerer, M.; Wolf, H. C. *Chem. Phys.* **1975**, *9*, 445.
(18) Kim, S. S.; Weissman, S. I. *Chem. Phys.* **1978**, *27*, 21.

0022-3654/87/2091-4851$01.50/0